# Identifying the Sources of Convective Memory in Cloud-Resolving Simulations

Maxime Colin, Steven Sherwood, Olivier Geoffroy, Sandrine Bony, David Fuchs

# Identifying the Sources of Convective Memory in Cloud-Resolving Simulations

MAXIME COLIN

*Climate Change Research Centre, and ARC Centre of Excellence for Climate System Science, University of New South Wales, Sydney, New South Wales, Australia, and Laboratoire de Météorologie Dynamique/IPSL, Sorbonne Université, UPMC Univ. Paris 06, CNRS, Paris, France*

STEVEN SHERWOOD

*Climate Change Research Centre, and ARC Centre of Excellence for Climate System Science, University of New South Wales, Sydney, New South Wales, Australia*

OLIVIER GEOFFROY

*Climate Change Research Centre, and ARC Centre of Excellence for Climate System Science, University of New South Wales, Sydney, New South Wales, Australia, and Centre National de Recherches Météorologiques, Météo-France/CNRS, Toulouse, France*

SANDRINE BONY

*Laboratoire de Météorologie Dynamique/IPSL, Sorbonne Université, UPMC Univ. Paris 06, CNRS, Paris, France*

DAVID FUCHS

*Climate Change Research Centre, and ARC Centre of Excellence for Climate System Science, University of New South Wales, Sydney, New South Wales, Australia*

(Manuscript received 29 January 2018, in final form 21 November 2018)

ABSTRACT

Convection is often assumed to be controlled by the simultaneous environmental fields. But to what extent does it also remember its past behavior? This study proposes a new framework in which the memory of previous convective-scale behavior, "microstate memory," is distinguished from macrostate memory, and conducts numerical experiments to reveal these memory types. A suite of idealized, cloud-resolving radiative–convective equilibrium simulations in a 200-km square domain is performed with the Weather Research and Forecasting (WRF) Model. Three deep convective cases are analyzed: unorganized, organized by low-level wind shear, and self-aggregated. The systematic responses to sudden horizontal homogenization of various fields, in various atmospheric layers, designed to eliminate their specific microstructure, are compared in terms of precipitation change and time of recovery to equilibrium. Results imply a substantial role for microstate memory. Across organization types, microstructure in water vapor and temperature has a larger and longer-lasting effect on convection than in winds or hydrometeors. Microstructure in the subcloud layer or the shallow cloud layer has more impact than in the free troposphere. The recovery time scale dramatically increases from unorganized (2–3 h) to organized cases (24 h or more). Longer-time-scale adjustments also occur and appear to involve both small-scale structures and domain-mean fields. These results indicate that most convective microstate memory is stored in low-level thermodynamic structures, potentially involving cold pools and hot thermals. This memory appears strongly enhanced by convective organization. Implications of these results for parameterizing convection are discussed.

## 1. Introduction

Understanding atmospheric moist convection is one of the main challenges to advance models used for climate projections, seasonal forecasts, and weather forecasts (Jakob 2014). These atmospheric general circulation

Supplemental information related to this paper is available at the Journals Online website: https://doi.org/10.1175/JAS-D-18-0036.s1.

*Corresponding author*: Maxime Colin, colinmaxime@hotmail.fr

DOI: 10.1175/JAS-D-18-0036.1

models (GCMs) have important shortcomings, and many of them are attributed to the convective parameterizations. GCMs rain too often and too little (Stephens et al. 2010). They tend to produce too much high cloud and too little shallow cloud (Chepfer et al. 2008; Sherwood et al. 2013). They can even produce cloud and precipitation responses to warming that have opposite signs (Stevens and Bony 2013). They struggle to represent a realistic diurnal cycle, although recent developments lead to improvements (Rio et al. 2009; Stratton and Stirling 2012; Bechtold et al. 2014; Folkins et al. 2014). They struggle to simulate the spatial organization of convection (Mapes and Neale 2011; Rowe and Houze 2015; Tan et al. 2015) and its temporal variability [e.g., Madden–Julian oscillation (MJO)] (Dai 2006; Waliser et al. 2009).

One prominent debate on convective parameterization concerned the ''quasi equilibrium'' hypothesis, which formed the basis for pioneering convective parameterizations (Arakawa and Schubert 1974; Arakawa 2004). Quasi equilibrium in this context means that convection is in equilibrium with the large-scale forcing: convective effects act to keep modifications of a closure variable (e.g., convective available potential energy) close to zero, compensating for large-scale processes. This is likely to be more accurate on longer spatiotemporal scales (at least several hours or 1 day).

A similar but weaker and more fundamental assumption that has received much less scrutiny is the ''diagnostic assumption'', made in most convective parameterizations [see subsections 5b and 5c in Arakawa (2004)], observational analyses (e.g., Masunaga 2012; Tan et al. 2013; Davies et al. 2013a), and many modeling studies (e.g., Kuang 2010). For convection, this assumption states that convective effects at a relatively large scale (and at time $t$) can be diagnosed at all from the state variables at that scale (and at the same time). Convective schemes that involve a separate triggering of convection generally do not assume quasi equilibrium (Emanuel 1991; Yano and Plant 2012b), since a triggering condition must be met before allowing convection to respond to the forcing. However, they usually do diagnose both the triggering and closure variables from the current gridscale state: they still make the diagnostic assumption.

But it is far from clear that the diagnostic assumption is justifiable. Many smaller-scale processes, which generally have their own internal time scales, bring inertia to the system. In a model for example, a diagnostic relationship effectively assumes that all such time scales are no longer than the model time step, which is typically of order 10 min in GCMs. Yet the time for a single updraft to penetrate the troposphere is longer than this. Moreover, the current trend is for models to have finer grid spacing and shorter time steps, so that this diagnostic assumption is increasingly problematic. This problem is already partly discussed in Bougeault and Geleyn (1989).

In a model, to go beyond the diagnostic assumption, one would need to add one or more prognostic variables to carry information (''memory'') on the previous behavior of unresolved processes. If convection were to be diagnosed by an equilibrium with the large-scale forcing, it would only be sensitive to the recent history of the forcing. With a prognostic formulation, not only do we have nonequilibrium convection, but convection is also made sensitive to its own history.

A few examples of such schemes exist. To our knowledge, the first was the scheme by Randall and Pan (1993) or Pan and Randall (1998). Their prognostic variable is the cumulus kinetic energy (CKE), whose source is taken to be the product between the cloud work function and the cloud-base mass flux. Other attempts to design a prognostic closure chose a variety of variables to become prognostic: convective vertical velocity and convective area fraction (Chen and Bougeault 1993), probability of undiluted updraft (Piriou et al. 2007), ''ORG'' variable for the spatial organization of convection (Mapes and Neale 2011), convective vertical velocity (Guérémy 2011), recent surface precipitation bucket (Willett and Whitall 2017), cold pool thermodynamic and geometric properties (Qian et al. 1998; Grandpeix and Lafore 2010; Del Genio et al. 2015), and cold pools and mesoscale organized flows (Park 2014). The sources feeding such prognostic variables include precipitation evaporation, buoyancy, surface precipitation, and downdraft mass flux and associated cooling and moistening. Cloud spacing could also be important (Cohen and Craig 2004).

While these efforts are important, they have not led to a consensus on whether memory needs to be explicitly included in models or how to do it. The current study is intended to be a step toward establishing more generally whether memory is important and how it might best be represented.

We define convective memory as the dependence of convective behavior on its own history, for given current large-scale (i.e., external or ''environmental'') conditions. This is broadly consistent with Davies et al. (2009) who define it via cloud life cycles. By analogy with statistical physics, one can define a microstate (description of all elementary units) and a macrostate (description of the collective behavior) for convection. In accord with this analogy, let $\lambda$ be a typical length scale of the system {e.g., typical GCM grid spacing [$O(100)$ km]}. We refer to the state variable fluctuations below the scale $\lambda$ as the *microstate*. The mean state at the scale $\lambda$ is referred to as the *macrostate*. Finally, the atmospheric state at a scale larger than $\lambda$ is referred to as the *synoptic state*. System memory can reside at each of these three scales: we

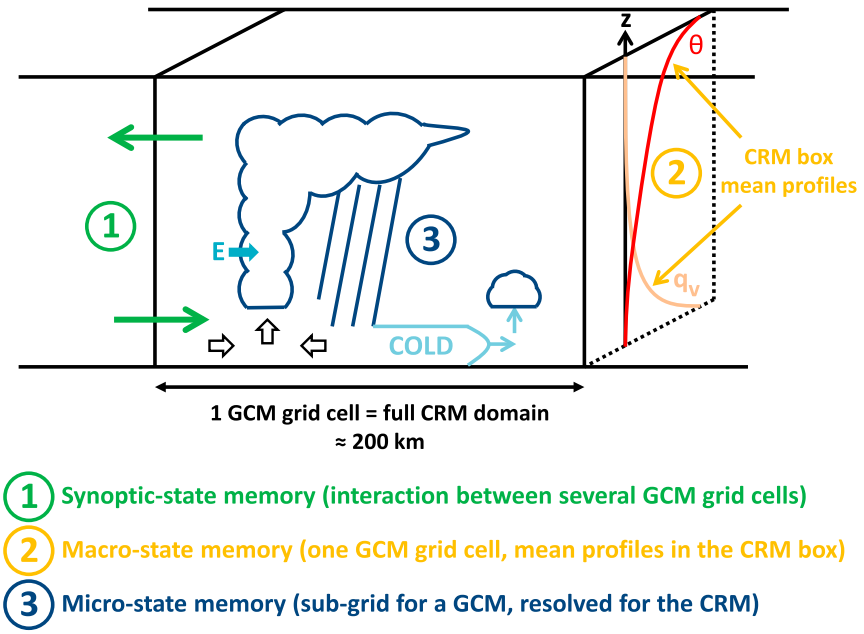


FIG. 1. Schematic of the three different types of memory that can emerge with respect to a mesoscale $\lambda$ (which may be a finite model resolution, but also more generally any length scale). Limited resolution may stem from the GCM grid cell (equivalent to a full CRM domain). Number 1 refers to synoptic state memory: it arises from processes that involve several GCM grid cells (such as synoptic-scale convergence/divergence, the Hadley circulation, or convective instability of the second kind). Number 2 refers to macrostate memory: it arises from processes that impact the local profiles of a single GCM grid cell (i.e., the mean profiles of the full CRM box; e.g., the mean profiles of specific humidity and potential temperature). Number 3 refers to microstate memory: it arises from GCM subgrid-scale processes (i.e., resolved CRM processes; e.g., rain evaporation, cold pools, secondary triggering of convection by cold pools, cloud entrainment, and convergence under the cloud base). Current GCMs resolve the synoptic-state memory through circulation, and the macrostate memory through convective parameterization. However, they are generally blind to microstate memory.

distinguish between microstate memory stored in microstate structures, macrostate memory stored in macrostate structures, and synoptic state memory stored in synoptic state structures (Fig. 1), although we do not consider the synoptic-state memory further in this study.

When $\lambda$ becomes smaller, individual unit effects start to be seen at the macrostate, and we would expect a nonequilibrium description of the microstate to be increasingly necessary to explain the macrostate. However, the overall effect of resolution on microstate memory is unclear since there are competing effects (cloud sample size decreases, but so does the number of unresolved processes). In contrast, reducing the time step clearly makes memory more important.

Microstate memory can be more precisely defined in terms of conditional probabilities. At each time $t$, let us define a measure of the convective state $C(\lambda, t)$ and a measure of the large-scale variables $\xi(\lambda, t)$. If convection had no microstate memory, the convective state $C(\lambda, t_0)$ would be conditionally independent from earlier convection $C(\lambda, t)\ \forall\, t < t_0$, given the large-scale state $\xi(\lambda, t_0)$. Microstate convective memory is the dependence of the PDF of $C(\lambda, t_0)$ on its own history, for given environmental conditions $\xi(\lambda, t_0)$.

Though convective memory as defined above will make convection more persistent, persistence alone does not establish memory: even if $C(\lambda, t)$ shows persistence, this could be due to persistence of $\xi(\lambda, t)$, itself arising for whatever reason.

Nonetheless, since memory should contribute to autocorrelation in time, convective memory may be viewed as strongly related to organization of convection in time. Furthermore, spatial convective organization is widely recognized as a key aspect of convective processes, more recently in simulations of self-aggregation (Bony et al. 2015; Wing et al. 2017) but for many years in studies motivated by observed organization where background wind shear plays an important role (e.g., Moncrieff 1981; Rotunno et al. 1988). Thus, we want to investigate the link between organization in time (memory) and organization in space (Davies 2008; Mapes and Neale 2011; Moseley et al. 2016).

The approach for identifying convective memory proposed here is based on the response of convection simulated by a cloud-resolving model (CRM) for a domain size $\lambda$ comparable to a typical global-model grid cell. We first introduce the methods (section 2). We then present results on the main variables and atmospheric layers where convective memory resides, and we examine the role of convective organization (section 3). Finally we summarize the results and discuss potential consequences for parameterization of convection (section 4).

## 2. Methods

### a. The simulations

For simplicity, this study uses control simulations in radiative–convective equilibrium (RCE). RCE provides a test bed for assumptions about convection and memory: if the assumptions are good, they should hold in RCE.

To assess convective memory in a wide range of situations, we conduct simulations of several convection types:

- The ''unorganized'' case. It is run with fixed sea surface temperature (SST), interactive surface fluxes, and no wind shear. The convection is not organized.
- Unorganized case with fixed surface fluxes. Latent and sensible surface fluxes are held uniform in space and constant in time, to the average values in the RCE state of the unorganized control run.
- Wind shear organized case. A wind, linearly varying with height (uniform shear), is imposed between heights of 0 and 4 km, by a moderate relaxation applied only to the domain-mean horizontal wind value. The imposed wind profile is $0\,m\,s^{-1}$ at the surface, and $20\,m\,s^{-1}$ at 4 km and above. This is similar to what was used in some previous studies (Robe and Emanuel 2001; Anber et al. 2014).
- Self-aggregated case. To get self-aggregation in the model, it was necessary to choose different turbulence and microphysics schemes (see section 2b).

In each case, simulations are spun up to an RCE state and then perturbed away from RCE to observe the response.

The unorganized case leads to scattered (''popcorn'') convective cells (Fig. 2). Overall, the mean RCE profiles (see the online supplemental material) resemble those obtained in previous studies (e.g., Romps 2011). They also compare well with the humidity profiles obtained from observations by radiosondes over the ocean, by Liu et al. (1991). In the case with imposed wind shear, convection creates elongated anvils parallel to the shear, with only one or two large convective cores in the domain. This creates a single large cold area near the surface, fed by several downdrafts. In the self-aggregated case, convection self-aggregates into a humid region surrounded by extremely dry areas in about 20 days.

### b. Model and setup

We use the Weather Research and Forecasting (WRF) Model, version 3.6, in its Advanced Research WRF (ARW) form (Skamarock et al. 2008; Wang et al. 2014) and in its ''idealized test'' framework. WRF-ARW dynamics solves the fully compressible, Euler nonhydrostatic equations. We hereby present 3D simulations.

We use doubly periodic boundary conditions, and a fixed SST of 302 K (except in the fixed-surface-flux case). The horizontal domain size is $202 \times 202$ points, and the horizontal grid spacing is 1 km. The vertical grid consists of 69 levels, going from the flat ocean surface up to the model top, which is about 30 km. We use a stretched vertical grid spacing: the vertical distance between two consecutive levels starts from 30 m near the surface, increases to 100 m near the cloud base, stays at 400 m in most of the free troposphere, reaches 500 m near the tropopause, and further increases to 2 km near the model top. The Coriolis parameter $f$ is set to zero.

In terms of dynamical options, we choose an implicit gravity wave damping layer (sponge layer) for vertical velocity in the top 5 km of the model. We also use full diffusion in physical space. A 3D prognostic equation for turbulent kinetic energy (TKE) is used to calculate turbulent eddy fluxes via a $K$ coefficient based on TKE, except for the self-aggregation case where the 3D Smagorinsky turbulence scheme is used instead. The influence of the turbulence scheme on self-aggregation has been investigated by Tompkins and Semie (2017).

The physical parameterizations include the Yonsei University boundary layer scheme, and a revised MM5 surface layer scheme based on Monin–Obukhov theory for computation of surface heat and moisture fluxes. There is no need to impose a minimum wind for surface flux calculations in this scheme (Jiménez et al. 2012). No cumulus parameterization is used. To be general, we choose a microphysical scheme with intermediate complexity and allowing for unorganized convection for most of our simulations: the WRF single-moment 6-class microphysics scheme (WSM6) (Hong and Lim 2006). We replace it by the Thompson microphysics scheme for the self-aggregated convection case, as tests showed that this scheme always produces strong self-aggregation. However, we could not use this latter scheme in all our cases, since it does not lead to unorganized convection with the desired model configuration. Explaining the sensitivity of self-aggregation to the microphysical scheme would require further study.

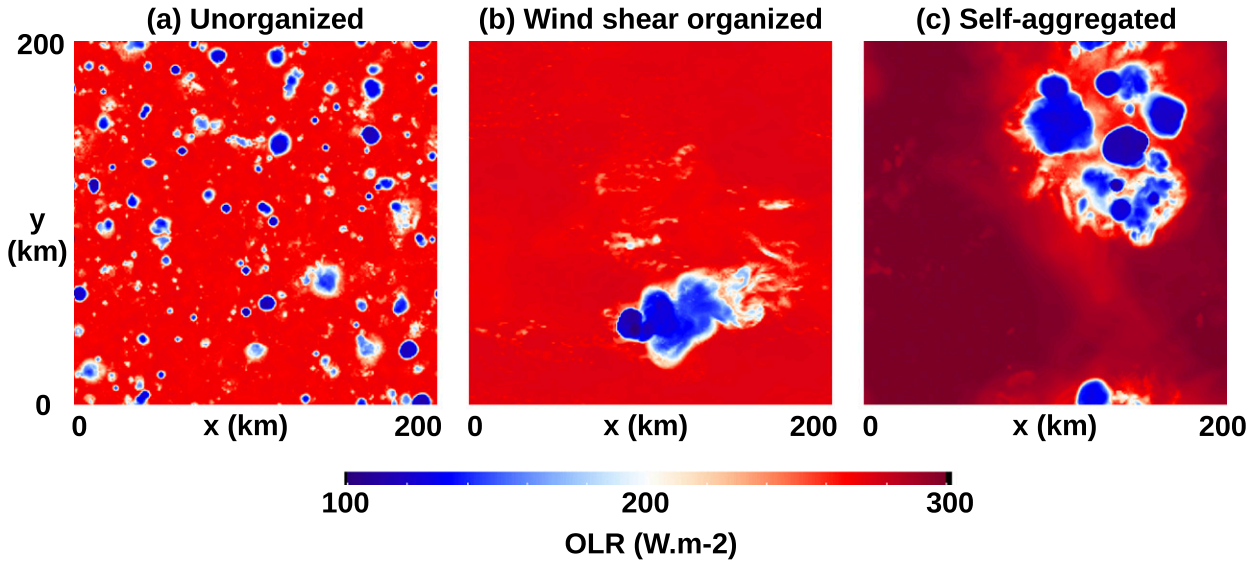


FIG. 2. Snapshots of outgoing longwave radiation (OLR) in the domain, in the radiative–convective equilibrium state, toward day 80 or 81 of the control runs, for three convective types with different convective organization: (a) unorganized case; (b) wind shear organized case, with the wind shear being positive and along the $x$ axis; and (c) self-aggregated case.

Sensitivity tests confirmed that choosing a different microphysical scheme does not change memory significantly, provided convective organization can be kept similar (see the online supplemental material).

We use interactive radiation, with the RRTMG schemes for both longwave (LW) and shortwave (SW) radiation. For simplicity we remove the diurnal cycle by making the cosine of the solar zenith angle constant at 0.8 (following Cronin 2014), and by decreasing the solar constant to 544 W $m^{-2}$, applying the usual mean insolation calculation to the equator rather than to the whole Earth (see the online supplemental material).

### c. Other simulation settings

For the spinup to RCE in the unorganized control run, the initial profiles for temperature and water vapor are chosen as the default initial sounding in the RCE test case available in WRF v3.7.1. There is no initial wind (even in the wind shear case). During initialization, random temperature perturbations (white noise) of up to 3-K amplitude are added in the first 2.5 km. These initial profiles do not matter much since we only consider the RCE state in the rest of the study.

The runs are performed for 80–100 days, with about 30 days of spinup time required to reach statistical RCE as measured by the mean precipitable water (Tompkins and Craig 1998). To be conservative we skip the first 2 months of each control simulation before initiating any experiments.

Following Held et al. (1993) and Wang and Sobel (2011), a light nudging toward zero (or toward the imposed shear, in the shear case) is imposed on the domain-mean horizontal winds. We do not expect the light nudging toward zero to significantly affect results.

### d. Design of perturbation experiments

To reveal convective memory, we impose instantaneous changes to the WRF microstate without changing the macrostate. Our experiments use a very simple kind of perturbation: horizontal averaging (hereby called ''homogenization'') of a given subset of prognostic state variables on model levels, at a selected time step. Then the model is restarted from these partly homogenized conditions with no other changes. We compare the evolution of convection following perturbations of different prognostic variables (or sets of variables) to that with no perturbation applied (control). We perturb all prognostic variables in WRF, namely, potential temperature, water vapor mixing ratio, hydrometeor mixing ratios, 3D winds, geopotential, column-integrated dry air mass, and TKE (see Table 1).

Usually, CRM studies perturb the macrostate (the forcing), and observe the time scale of the response (Kuang 2010; Raymond and Herman 2011). The recovery in this case involves feedbacks between convection and macrostate, so could be slow because of long macrostate memory, even in absence of microstate memory (i.e., even if convection adjusts instantly to the macrostate). To minimize this issue and reveal microstate memory instead, our homogenization perturbations do not affect the macrostate, only the microstate.

The RCE state varies in time because of chaotic internal variability. Consequently, as in previous studies (Cohen and Craig 2004), we ensure statistically significant results by constructing ensembles, repeating each experiment at 5–20 different restart times taken from the RCE state reached by each convective case. Uncertainty is then found to be very small.

## 3. Results

If convection were purely related to the macrostate via a diagnostic relationship, it would resume as before very rapidly. Here we therefore take the time required for recovery as a measure of microstate memory. Also, by eliminating particular microstate structures, homogenization should erase any corresponding microstate memory, thus moving the system further away from RCE. We therefore take the magnitude of this departure as a second measure of microstate memory. Here, convection intensity is quantified via domain-averaged precipitation.

### a. Convective organization and memory

Convective organization leads to a dramatic increase in convective memory, particularly acute with self-aggregation. The recovery time scale for water vapor experiments is 1 h for unorganized convection, 6 h for convection organized by wind shear, and more than 24 h for self-aggregated convection: convective organization enhances memory by a factor of up to 25 (Fig. 3). Also, in the self-aggregated case, precipitation remains zero for 12 h after homogenizing, whereas in the unorganized case, it does not even reach zero. With self-aggregation, the precipitation response amplitude when homogenizing temperature (28 mm day$^{-1}$) is about 8 times as large as in the unorganized case (3.5 mm day$^{-1}$). Sensitivity tests confirmed that these memory changes are due to organization, not to the choice of microphysical scheme (see the online supplemental material).

To explain why organized convection shows so much more memory, we can assess the domain-mean value of convective available potential energy (CAPE) in the equilibrium state of the different organization cases. The CAPE is computed at each point pseudoadiabatically by lifting the air parcel with the maximum equivalent potential temperature in the first 3 km then averaging horizontally. The average CAPE is highest in the unorganized state (3200 J kg$^{-1}$), intermediate in the case organized by wind shear (2350 J kg$^{-1}$), and lowest in the self-aggregated case (750 J kg$^{-1}$). With more organized convection, the CAPE is smaller, so it takes longer to regenerate locally the greater amount of convective instability needed to restart convection from scratch. This is likely to explain why it takes longer to recover from homogenization.

TABLE 1. List of variables averaged in the homogenization experiments. The model is restarted from different combinations of horizontally homogenized variables. The variables $q_c$,$q_r$,$q_i$,$q_s$, and $q_g$ refer to the mixing ratios of cloud liquid water, rain, ice, snow, and graupel, respectively.

| Symbol | Variable |
|---|---|
| $q_v$ | Water vapor mixing ratio |
| $\theta$ | Potential temperature |
| **u** | 3D winds ($u$, $v$, $w$) |
| $q_{\text{cond}}$ | All hydrometeors ($q_c$,$q_r$,$q_i$,$q_s$,$q_g$) |
| PH | Geopotential |
| MU | Dry air mass in the vertical column |
| TKE | Turbulent kinetic energy |

Another explanation is that homogenization is a stronger perturbation when there are stronger structures to be homogenized. Self-aggregation generates very large contrasts in humidity across the domain, and therefore a large variance of atmospheric fields. Likewise, shear-organized convection has larger conversion of horizontal momentum to vertical momentum, and thus larger turbulence and associated variance.

### b. In which variables is convective memory stored?

Preliminary experiments showed that geopotential, column dry air mass, and subgrid TKE did not contribute to convective memory (see the online supplemental material). Therefore, we focus our analysis on the role of the other prognostic variables that could be important for memory: winds, hydrometeors, water vapor, and temperature.

The ''single set'' experiments (Fig. 3) show that the amplitude of the precipitation response is larger when temperature or water vapor are homogenized than when winds or hydrometeors are homogenized, indicating that thermodynamic heterogeneities are more important than wind and hydrometeor heterogeneities. In the unorganized case (Fig. 4), temperature homogenization leads to a recovery time scale of about 1.5 h, 1 h for water vapor homogenization, and 1.5 h for wind homogenization, while for the hydrometeors the recovery time scale is about 20 min. The response to homogenizing the hydrometeors has a large amplitude but rapid time scale, indicating that while homogenizing the hydrometeors impacts the precipitation initially, they are not important for memory. These results are statistically robust since the standard error of the mean around the ensemble means is always very small.

In the shear-organized case (Fig. 5), water vapor still carries the most memory and hydrometeors still play a negligible role. But the winds become a more important

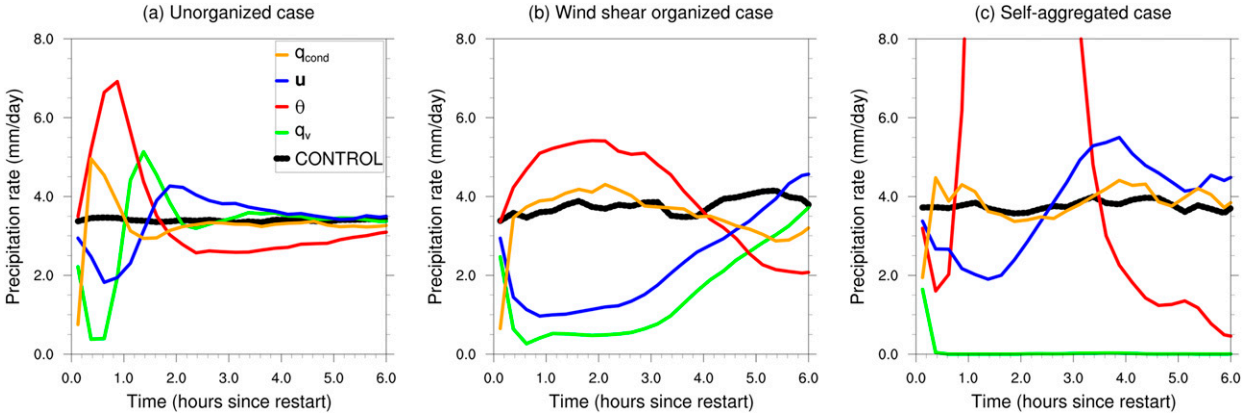


FIG. 3. Response of horizontally averaged precipitation rate after homogenization and model restart, for the control run and for experiments on a single variable; colors indicate different experiments, and the legend indicates the variable homogenized in each experiment (see Table 1). These are ensemble averages over 19 or 20 members. The panels represent experiments conducted on different convective types: (a) unorganized convection, (b) convection organized by wind shear, and (c) self-aggregated convection. The peak precipitation rate following homogenization of temperature in the self-aggregated case (off scale) is 32 mm day$^{-1}$.

source of memory than temperature, probably because the winds are what organizes the convection.

In the self-aggregated case (Fig. 6), there is a dramatic increase in memory residing in the thermodynamic variables: mostly water vapor (>24 h), but also temperature (~13 h). The hydrometeors still do not store any memory. With self-aggregation, water vapor and temperature prevail by more than an order of magnitude over dynamics and microphysics for memory storage. This is consistent with the fact that, in the self-aggregated case, a strong contrast in humidity develops between wet and dry subdomains, which does not develop nearly as strongly with disorganized convection or wind shear organized convection.

The smaller memory storage of the dynamical variables (3D winds) compared to the thermodynamic

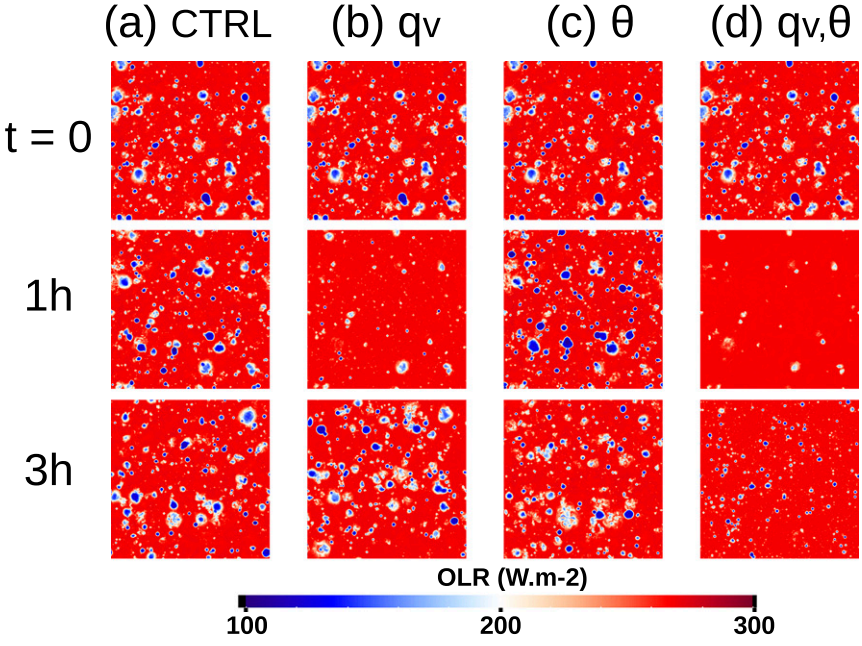


FIG. 4. Snapshots of the OLR response to various homogenization in the unorganized case. (a) The control run, (b) water vapor homogenization, (c) potential temperature homogenization, and (d) water vapor and potential temperature homogenization. (top to bottom) Times are at $t$ = 0, 1, and 3 h after homogenization.

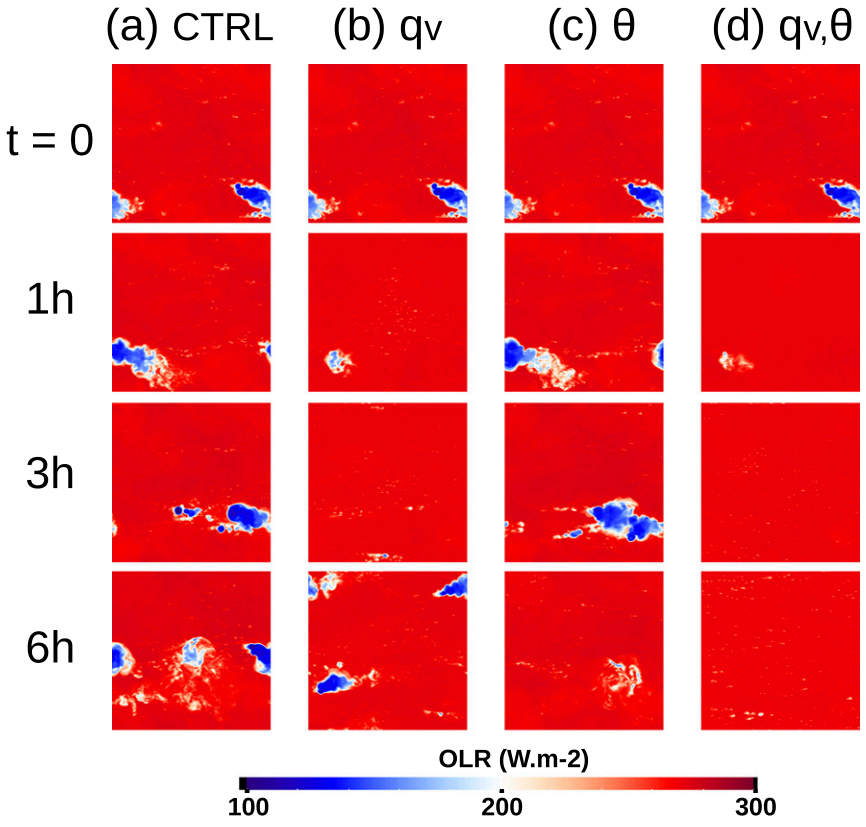


FIG. 5. As in Fig. 4, but for the wind shear organized case. (top to bottom) Times are at $t = 0$, 1, 3, and 6 h after homogenization.

variables is confirmed by the "double set" experiments (Fig. 7). In the unorganized case, homogenizing winds and water vapor together has a similar impact as homogenizing water vapor only. Likewise for winds and temperature together. However, homogenizing both water vapor and potential temperature together leads to a recovery time scale that is twice as long (2.5 h) as when only one thermodynamic variable is homogenized (~1 or 1.5 h).

In the wind shear organized case, the combination of water vapor and temperature still carries more memory than the combination between winds and either of the thermodynamic variables. Homogenizing water vapor and winds together leads to the same response as homogenizing water vapor only, while homogenizing both temperature and winds leads to an intermediate response more similar to wind only. These results show that winds and temperature are important, but winds are now the secondary storage of convective memory after water vapor.

The self-aggregated case shows similar results in terms of the relative importance of variables, but with much greater memory overall. When both water vapor and temperature are homogenized, the combined effect is the largest of all experiments: precipitation remains zero for about 18 h.

### c. *Moist static energy interpretation*

In most experiments, precipitation is reduced after homogenization. There is one exception, however, when temperature is homogenized.

In most experiments the standard deviation of moist static energy (MSE) near the surface (and to a lesser extent at 500 hPa) is reduced in the first few hours after homogenizing (Fig. 8). Also, the standard deviation of MSE in the subcloud layer reacts earlier than precipitation (see also Fig. 3a), which suggests causality. The standard deviation of MSE is the most strongly reduced by homogenizing water vapor, and it is precisely the experiment in which convection is the most strongly reduced. Conversely, homogenizing temperature leads to an increase in the standard deviation of MSE instead of a decrease.

To explain this result, we note that raining locations are associated with cold pools, which means they are usually colder in the boundary layer than the nonconvective locations. When homogenizing temperature, the MSE of wet convective areas thus becomes even higher than before homogenization, therefore, enhancing the standard

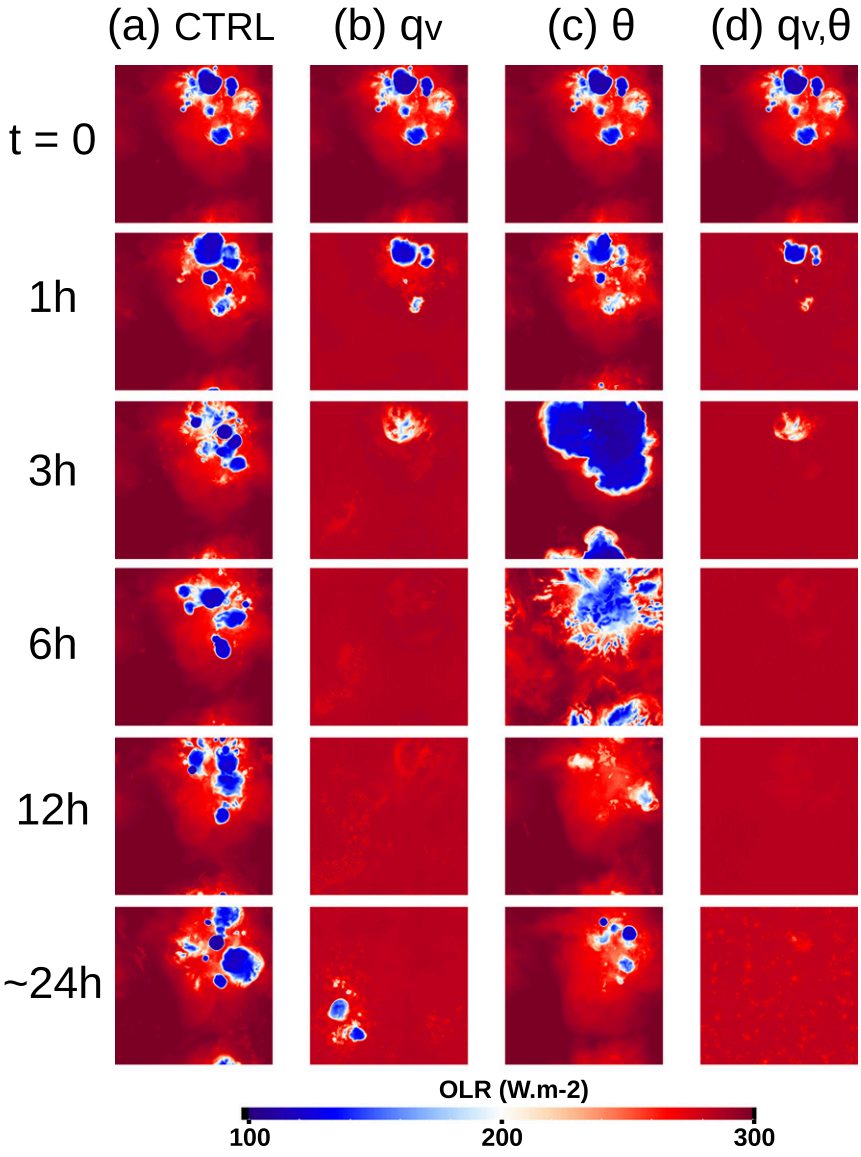


FIG. 6. As in Fig. 4, but for the self-aggregated case. (top to bottom) Times are at $t = 0, 1, 3, 6, 12$, and about 24 h after homogenization.

deviation of boundary layer MSE and intensifying convection. So microscale MSE structures in the boundary layer are the key for convective evolution here.

In the self-aggregated case, there is a short-term decrease in precipitation (~45 min) when temperature is homogenized, which is quickly superseded by the precipitation increase observed in the other cases (Fig. 3). After homogenizing temperature in the self-aggregated case, the cloudy area is not only much warmer in the subcloud layer, but also slightly warmer in the shallow cloud layer. This increases the saturated water vapor mixing ratio, so that it becomes harder to create clouds: cloud mixing ratio and rain mixing ratio slightly decrease in the shallow cloud layer of the convective region just after homogenizing.

Previously aggregated convection usually recovers to another self-aggregated state after homogenization, but not always (Fig. 6). If only water vapor or temperature is homogenized, convection clearly recovers to an aggregated state. However, if both are homogenized, it recovers in a practically unorganized state, although slightly aggregated, probably due to the persistence of wind (and perhaps hydrometeors) structures. It is important to note where aggregation recovers: at the original location when temperature is homogenized, but in the opposite part of the domain when water vapor is homogenized. This is

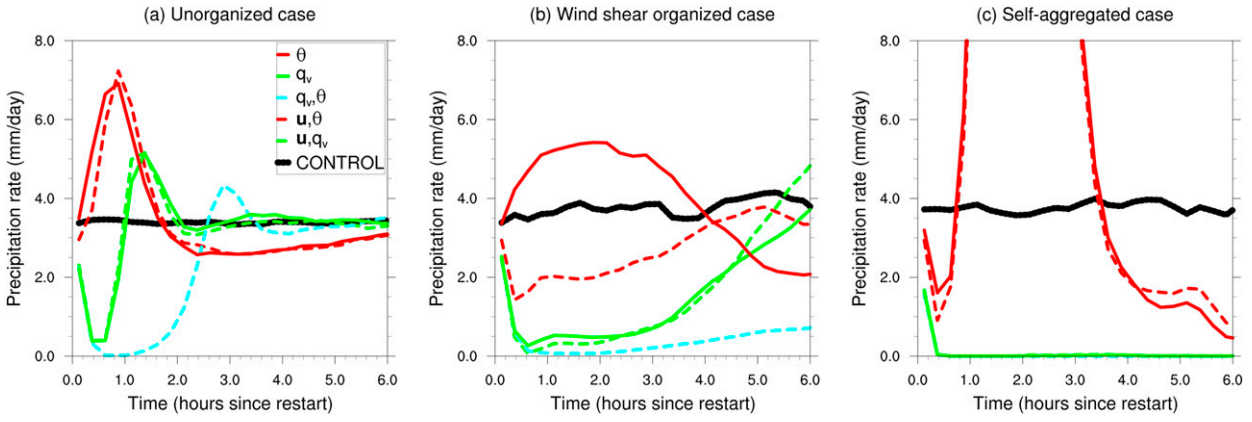


FIG. 7. Response of horizontally averaged precipitation rate after homogenization and model restart, for the control run and for experiments on a double set of variables (dashed), compared to the single-variable temperature and humidity results (solid). Different experiments are indicated by different colors (see legend and Table 1). These are ensemble averages over 19 or 20 members. The panels represent experiments conducted on different convective types: (a) unorganized convection, (b) convection organized by wind shear, and (c) self-aggregated convection.

consistent with the modifications of subcloud layer MSE in convective and dry regions caused by homogenization: self-aggregation occurs where the subcloud MSE is the largest. The subcloud MSE gradients are primarily due to humidity gradients, so that before homogenization, convective areas have a higher MSE (higher humidity despite lower temperature). This remains the case after temperature is homogenized, but it is inverted when water vapor is homogenized.

### d. *Which layer of the atmosphere carries most memory?*

The results from section 3c suggest an important role for the boundary layer. To go one step further, we carry out experiments where we homogenize variables only in one specific layer at a time: the subcloud layer [surface–940 hPa (~600 m)], shallow cloud layer/midtroposphere (940–700 hPa), or free troposphere (700 hPa–tropopause). Following the previous results, for these experiments we only average the thermodynamic variables: water vapor and temperature.

In the unorganized case, the precipitation recovery time scale is largest when the subcloud layer is homogenized (Fig. 9a). In contrast, the amplitude of the response is almost zero when homogenizing the free troposphere. Thus, memory mostly resides in the subcloud layer.

The shallow cloud layer appears to contribute as a secondary storage of convective memory compared to

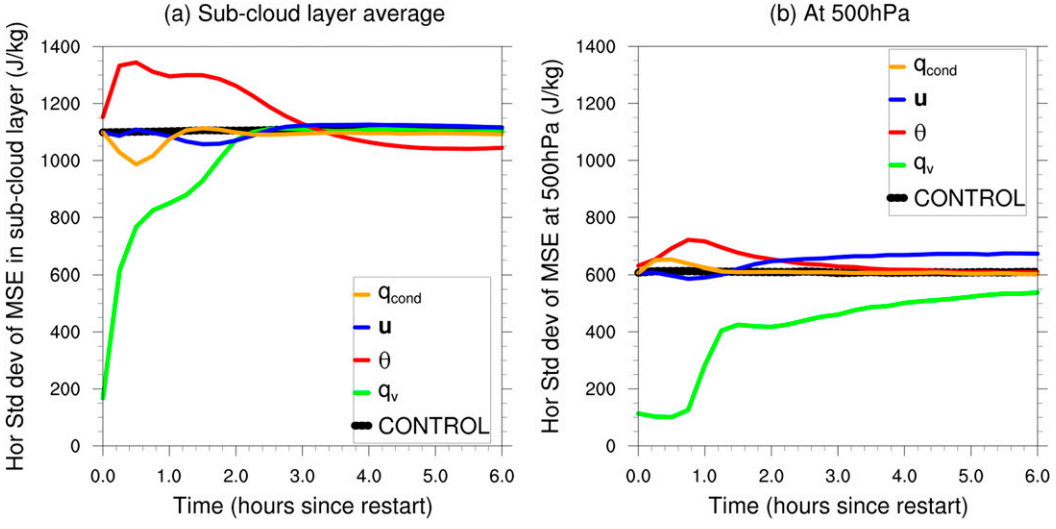


FIG. 8. Response of microscale structures, for different 3D experiments in the unorganized convection case. Different experiments are indicated by different colors (see legend and Table 1). Both panels show ensemble averages for 19 members. (a) Sub-cloud-layer average of the horizontal standard deviation of MSE. (b) Horizontal standard deviation of MSE at 500 hPa.

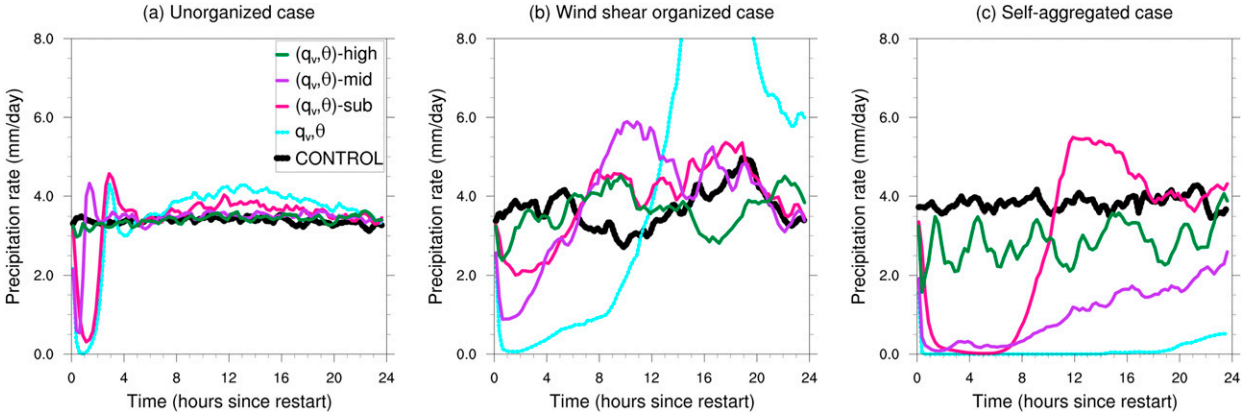


FIG. 9. Response of horizontally averaged precipitation rate after homogenization and model restart, for the control run and for experiments on specific layers only: homogenization before the restart is conducted over different atmospheric layers: subcloud layer (surface–940 hPa), midlayer (940–700 hPa), and high layer (700 hPa–tropopause). Different experiments are indicated by different colors (see legend and Table 1). These are ensemble averages over 19 or 20 members. Different panels represent experiments conducted on different convective types: (a) unorganized convection, (b) convection organized by wind shear, and (c) self-aggregated convection.

the subcloud layer. The response time scale for homogenization of this layer is only 1 h, compared to the 2.5-h time scale for the subcloud layer.

The shallow cloud layer impacts precipitation on relatively shorter time scales since homogenizing this layer will directly impact clouds. The subcloud layer has a longer lasting impact since it takes more time for the air in the subcloud layer to generate updrafts, clouds, and then precipitation.

In the case with wind shear, the relative role of the shallow cloud layer is stronger than in the unorganized case, but not as strong as in the self-aggregated case (Fig. 9c).

In the self-aggregated case (Fig. 9), as in the two other cases, most memory still comes from the lowest two layers: the subcloud and shallow cloud layers. The free troposphere (700 hPa–tropopause) still plays a much weaker role, although a little stronger than for the other cases, since there are slightly stronger structures in the free troposphere in the self-aggregated case (stronger differences between the convective and the dry regions). The main difference is that the memory coming from the subcloud layer is dominant in the unorganized case (by a factor of 2 in recovery time scale), but it is the memory coming from the shallow cloud layer that is dominant with self-aggregation (also by a factor of about 2). In comparison, the memory coming from these two low layers is almost equivalent in the wind shear organized case (the recovery time scales are the same).

### e. *Negligible role of surface fluxes*

In section 3d we found that the sub-cloud-layer thermodynamical variables are the main source of convective memory. Since this layer is in contact with the surface, it raises the question of whether part of the long recovery might be due to the surface fluxes (either to their average or to their microscale fluctuations). We investigate this using the fixed surface flux experiments (section 2a).

The results (see the online supplemental material) are almost identical to those with fixed SST. With fixed surface fluxes the amplitude of the response is very slightly smaller, but otherwise, it is the same. We draw two conclusions. First, surface flux heterogeneity is not a source of microstate convective memory. Second, the macrostate surface–flux feedback does not play a significant role in helping the system regain its RCE state.

### f. *Secondary response: A microstate–macrostate feedback*

In some of our experiments, there is a longer-term secondary response, which usually has the opposite sign compared to the initial response. For example for unorganized convection, see the experiment on $\theta$ and $q_v$ together in Fig. 9a (where there is a 24-h secondary response time scale), or experiment on $\theta$ (7-h time scale) or winds (5-h time scale) in Fig. 3a. It appears that there is a feedback between the microstate response and the macrostate response. Systems in RCE have many modes of variability, since they exhibit various natural oscillations (Randall et al. 1994; Hu and Randall 1995; Yano and Plant 2012a). The homogenization experiments seem either to excite some particular modes of this dynamical system, or to trigger a damped oscillatory response.

In most experiments in the unorganized case, most variables recover to their RCE value after about 6 h. This is not true for the one where both water vapor and temperature are homogenized (Fig. 10), where the precipitation response starts a longer-period oscillation

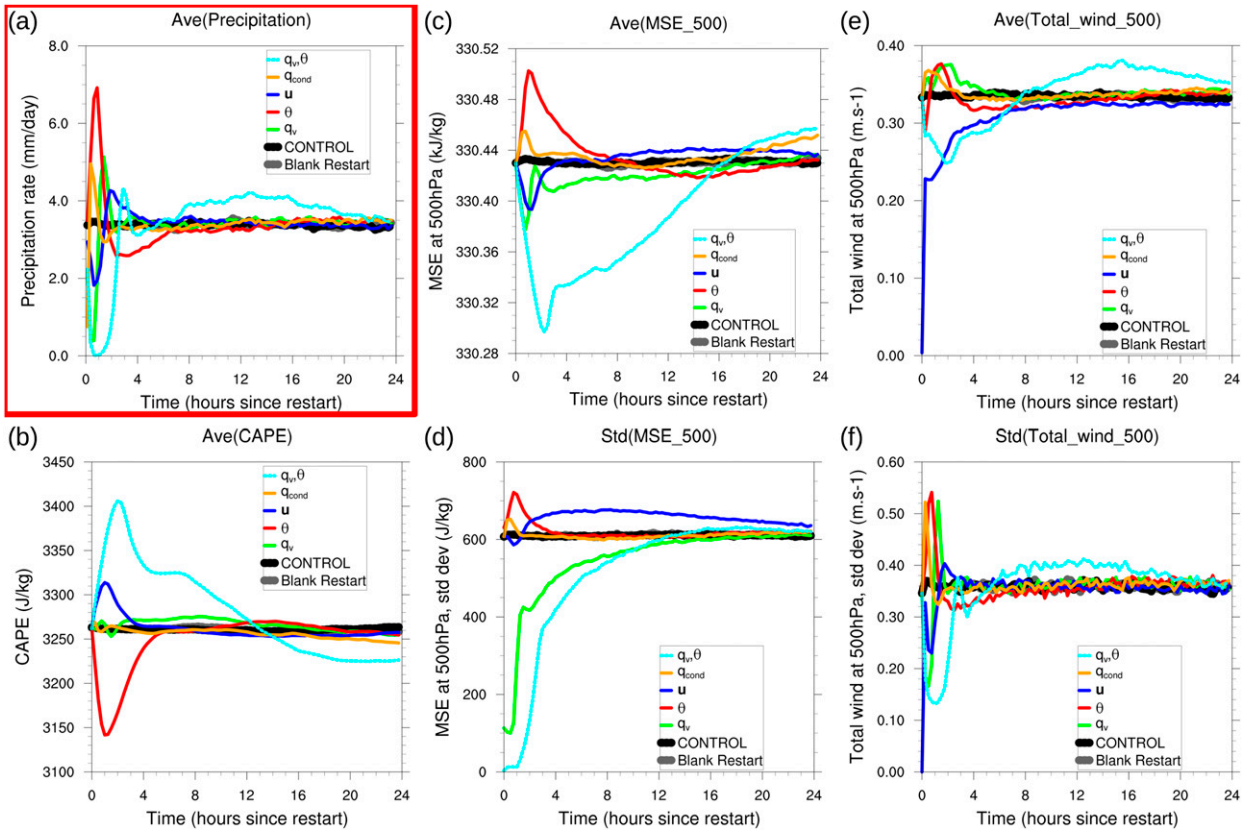


FIG. 10. Response after homogenization of variables given by the legend (colors, see Table 1) and model restart, on longer time scale (24 h), for unorganized convection. These are ensemble averages over 19 members. The response of different variables is presented: (a) horizontal average of precipitation rate, (b) horizontal average of CAPE, (c) horizontal average of MSE at 500 hPa, (d) standard deviation of MSE at 500 hPa, (e) horizontal average of the total wind at 500 hPa, and (f) standard deviation of the total wind at 500 hPa. As shown by the legend, the lines show the control run (black); single-set homogenization experiments on water vapor (green), potential temperature (red), winds (dark blue), hydrometeors (orange); and a double-set homogenization experiment on water vapor and potential temperature together (dashed cyan). The total wind is computed as the amplitude of the 3D wind vector. The standard deviation of the total wind is very similar to the convective kinetic energy (CKE). Convective available potential energy (CAPE) and moist static energy (MSE) are also indicated. Note that here CKE refers to the CKE defined at each point by the velocities resolved by the CRM, which is different from the parameterized subgrid TKE used by the CRM.

away from equilibrium at 7 h, which peaks at 13 h. To explain this, note that after 6 h, even though precipitation has recovered to its RCE value, CAPE has not, showing that the macrostate after 6 h is different from the macrostate in RCE.

This secondary response should not influence our results on microstate memory too much since it is of smaller amplitude, and we are focusing on the first part of the response. We discuss a potential way to prevent interactions between the microstate and macrostate in section 3h.

### g. *Summary, discussion, and hints on processes*

Our results show that in all three convective organization types, water vapor is the primary storage of memory, followed by temperature (especially in the unorganized case) and then wind (especially in the case organized by wind shear). There is thus a dominant "water vapor memory." Moreover, memory is mostly stored at low levels. These results resonate with Stirling and Petch (2004) who showed in a 2D setup that the diurnal cycle of unorganized convection is most strongly affected by microscale variability of relative humidity in the boundary layer, and with Davies (2008) and Davies et al. (2013b). The importance of water vapor for convective memory is also consistent with its importance in self-aggregation (Tompkins 2001b).

We conclude that convective memory mostly resides in low-level thermodynamics, which provides hints about the processes involved. Cold pools and thermals are strong intrinsic thermodynamical microstate structures at low levels, and therefore good candidates for

processes leading to microstate memory. This is supported by the key role of cold pools in convective organization (Tompkins 2001a). This inference tends to support the development of prognostic cold pool schemes, which have been shown to bring memory to the system Del Genio et al. (2015). Further study of the controlling processes for memory would be helpful.

The dominant horizontal scales for memory were not investigated here, but it can be inferred from previous studies. Stirling and Petch (2004) showed that horizontal scales larger than 10 km have the largest influence on subsequent convection in an experiment representing the typical diurnal cycle. Similarly, Davies et al. (2013b) demonstrated that horizontal scales of 5–20 km are the most important for the memory. This is consistent with the typical 10–20-km scale of the cold pools simulated in the unorganized case.

### *h. General caveats*

In this study, feedbacks from the macrostate onto convection are not forbidden during convective recovery to RCE. Domain-mean temperature, humidity, and CAPE are allowed to vary with time, so the macrostate is not held fixed (Fig. 10). Thus, recovery of the microstate to homogenization involves interaction with the macrostate (e.g., increase of CAPE). So the responses measured here partly include macrostate memory. However, we conjecture that macrostate feedbacks affect all perturbations similarly, and on longer time scales, so that comparing the recoveries should still be valid. This conjecture is consistent with results by Davies et al. (2013b). Significant work would be required to completely get rid of the macrostate feedbacks, which calls for further study. A method to achieve this would be either to impose the macrostate or to statistically remove the effect of macrostate variations.

By changing the microphysical scheme, we strongly modified the convective organization in space. We confirmed that the dramatic change in memory is due to the change in organization, not just to the change in microphysical scheme, by evaluating the memory with the Thompson microphysics scheme but a very small domain that forces a relatively unorganized state. The results show that memory is similar to the unorganized case with WSM6 microphysics (see the online supplemental material).

Homogenization is a very strong perturbation to the microstate. So one could argue that our experiments may overestimate recovery times compared to, for example, replacing the convective microstate with a nonconvective one. We expect that the relative importance of the different sources of memory found in this simple approach, under different degrees of organization, would hold in more realistic approaches, although it will need to be tested in future work.

This study is performed in RCE, so there is no externally imposed large-scale forcing. This may limit the generality of our results. It would be interesting to check whether the results hold in an idealized atmosphere that undergoes a large-scale upward vertical velocity, representing the trough of a large-scale wave, and leading to higher precipitation rate. But even if RCE may neglect part of the complexity of the real atmosphere, it is still a useful framework to look at convection–circulation feedbacks.

We have analyzed the memory of tropical convection only. Potentially, the wind shear experiments may partly capture behaviors of synoptic weather systems in the extratropics.

Convective memory as considered in this study includes convection but also the resolved turbulence, since the homogenization technique acts on the whole microstate, independently from whether the microstate structures are more on convective length scales or on turbulent length scales.

### *i. Implications for parameterizations*

Overall, our results suggest that some of the previous studies have chosen reasonable memory storage through thermodynamic variables (e.g., precipitation evaporation, cold pools), even though some other studies may have given too much memory role to the dynamical variables (e.g., convective vertical velocity, subgrid-scale TKE or CKE) or to the microphysics. Even though these dynamical variables are likely to be ultimately controlled by the thermodynamic structures, they do not appear to be the main storage of memory themselves. Choosing precipitation as the storage of memory is probably not ideal, as there is no memory in the hydrometeors, even though precipitation is also controlled by many thermodynamic conditions. The use of precipitation evaporation might be relevant, as it strongly depends on the relative humidity of the subcloud-layer, which is a thermodynamical variable.

Still, few studies have directly chosen water vapor and temperature as a memory storage, apart from studies using cold pool thermodynamic profiles (Qian et al. 1998; Grandpeix and Lafore 2010; Park 2014; Del Genio et al. 2015). Hopefully this study will trigger more parameterization development based on these direct thermodynamic variables, for example, by a prognostic representation of the unresolved boundary layer thermodynamic structures (e.g., via spatial variance of water vapor and temperature, or of moist static energy). Finally, our results may help choose the prognostic variable in order to build a

convective parameterization with memory in an implicit way such as Mapes and Neale (2011).

For example, Del Genio et al. (2015) improved the representation of the Madden–Julian oscillation (MJO) by adding memory, which resides in prognostic cold pools. Their best MJO is simulated when the scheme has memory, but too much memory also degrades the MJO: what is needed is the right amount of memory.

## 4. Conclusions

This study introduces a framework to clarify previous discussions about convective memory, and uses CRM simulations to explore where it comes from. The new framework distinguishes at least two types of convective memory. Convection can remember its previous states through the impact of earlier convection on the current macrostate (large-scale state averaged on a scale $\lambda$ such as the local grid column in a GCM), which can feed back onto convection. This type of memory can in principle be captured by a GCM with an accurate diagnostic convection scheme (one that predicts convective effects based on the current macrostate). However, convection can also remember its previous state via persistence of the microstate itself, which is not resolved at the scale $\lambda$. Such *microstate memory* will not be captured by a convective scheme unless the parent model carries additional prognostic variables representing the microstate. To the extent that a given macrostate can be associated with a range of microstates, and that the microstate influences convection, then the microstate represents an additional degree of freedom for the convection that should be taken into account by convective parameterizations.

We show that microstate memory is indeed present, and is highly enhanced by convective organization: the amount of microstate memory is related to the magnitude of spatial inhomogeneities. Self-aggregated convection has the most memory, wind shear organized convection has intermediate memory, and unorganized convection has the least. Yet, even in the unorganized case, recovery of the RCE state after a microstate perturbation can require several hours, which is much longer than a GCM time step (~10–20 min). When convection is organized, such recovery can take longer than the diurnal time scale (24 h) in some cases. This finding strongly supports efforts to add prognostic variables (i.e., memory) into parameterizations. It also indicates that the degree of memory is very sensitive to the degree of spatial organization, so that a scheme capturing one may also capture the other.

The main sources of microstate memory are found to be water vapor, then temperature, and then winds. But the importance of winds increases with wind shear. The memory mostly comes from the lowest part of the atmosphere: the subcloud layer and the shallow cloud layer (up to 700 hPa). For unorganized convection the subcloud layer is the most important, while the shallow cloud layer dominates for wind shear organization and even more clearly for self-aggregation.

This suggests memory comes from processes that contribute to the spatial variance of low-level moist static energy (MSE) and/or make convection sensitive to it. This includes cold pools, hot thermals, and other rain-associated thermodynamic processes such as rain evaporation, and supports parameterizations coupling convection to these processes. Further study intended to specifically discriminate between processes that lead to convective memory would be helpful.

Physically, the persistence of microscale structures matters for convection since convection tends to localize on the maxima of subcloud layer MSE. Also, cold pools and local moistening by detrainment in the shallow cloud layer are microstate elements that favor nearby subsequent convection, increasing microstate memory.

To further understand the origins of microstate convective memory and to test how robust the results are, subsequent investigations could experiment with different kinds of perturbations, and assess the sensitivity to various model choices. In particular, we could use perturbations with spatial filtering to determine the scale of the structures storing memory. We could also test the sensitivity to a large-scale vertical velocity forcing. Moreover, it is unclear whether the large-scale vertical velocity, a macrostate variable, could indirectly capture the past microstate (and if so, to what extent and by which mechanism).

The study focuses on microstate memory: at this stage, we have not provided insight on sources of macrostate and synoptic state memory. Presumably, free-tropospheric water vapor could play an important role in the macrostate memory (Tompkins 2001b), as well as higher-tropospheric temperature (Raymond and Herman 2011), and this could be further clarified by expanding methods such as Kuang (2010) via introducing time lag. An overall target for GCMs could be to better represent these three types of memory, which all contribute to spatiotemporal variations of convection and precipitation (e.g., diurnal cycle, precipitation frequency).

Finally, this study reveals the link between memory and organization, which suggests that improved representation of convective memory might improve convective organization (Tobin et al. 2013), such as the Madden–Julian oscillation, or monsoons.

*Acknowledgments.* We thank Jean-Yves Grandpeix, Romain Roehrig, Christian Jakob, Alison Stirling, Catherine Rio, Frederic Hourdin, John Petch, Cathy Hohenegger, and Vishal Dixit for useful discussions; and

Shuguang Wang, Antonio Parodi, Martin Singh, Daniel Kirshbaum, Frank Robinson, and Jimy Dudhia for their expertise on WRF and cloud-resolving model settings. We also thank George Young for providing useful information. Finally we thank the three anonymous reviewers who provided insightful comments that improved the manuscript substantially. MC, SS, and DF were funded by the Australian Research Council CE110001028 and FL150100035. OG was funded by ARC DP140101104. Simulations were run on the Australian National Computational Infrastructure (NCI) supercomputer.

## REFERENCES

Anber, U., S. Wang, and A. Sobel, 2014: Response of atmospheric convection to vertical wind shear: Cloud-system-resolving simulations with parameterized large-scale circulation. Part I: Specified radiative cooling. *J. Atmos. Sci.*, **71**, 2976–2993, https://doi.org/10.1175/JAS-D-13-0320.1.

Arakawa, A., 2004: The cumulus parameterization problem: Past, present, and future. *J. Climate*, **17**, 2493–2525, https://doi.org/10.1175/1520-0442(2004)017<2493:RATCPP>2.0.CO;2.

——, and W. H. Schubert, 1974: Interaction of a cumulus cloud ensemble with the large-scale environment, Part I. *J. Atmos. Sci.*, **31**, 674–701, https://doi.org/10.1175/1520-0469(1974)031<0674:IOACCE>2.0.CO;2.

Bechtold, P., N. Semane, P. Lopez, J.-P. Chaboureau, A. Beljaars, and N. Bormann, 2014: Representing equilibrium and nonequilibrium convection in large-scale models. *J. Atmos. Sci.*, **71**, 734–753, https://doi.org/10.1175/JAS-D-13-0163.1.

Bony, S., and Coauthors, 2015: Clouds, circulation and climate sensitivity. *Nat. Geosci.*, **8**, 261–268, https://doi.org/10.1038/ngeo2398.

Bougeault, P., and J. F. Geleyn, 1989: Some problems of closure assumption and scale dependency in the parameterization of moist deep convection for numerical weather prediction. *Meteor. Atmos. Phys.*, **40**, 123–135, https://doi.org/10.1007/BF01027471.

Chen, D., and P. Bougeault, 1993: A simple prognostic closure assumption to deep convective parameterization: I. *Acta Meteor. Sin.*, **1**, 1–18.

Chepfer, H., S. Bony, D. Winker, M. Chiriaco, J.-L. Dufresne, and G. Sèze, 2008: Use of CALIPSO lidar observations to evaluate the cloudiness simulated by a climate model. *Geophys. Res. Lett.*, **35**, L15704, https://doi.org/10.1029/2008GL034207.

Cohen, B. G., and G. C. Craig, 2004: The response time of a convective cloud ensemble to a change in forcing. *Quart. J. Roy. Meteor. Soc.*, **130**, 933–944, https://doi.org/10.1256/qj.02.218.

Cronin, T. W., 2014: On the choice of average solar zenith angle. *J. Atmos. Sci.*, **71**, 2994–3003, https://doi.org/10.1175/JAS-D-13-0392.1.

Dai, A., 2006: Precipitation characteristics in eighteen coupled climate models. *J. Climate*, **19**, 4605–4630, https://doi.org/10.1175/JCLI3884.1.

Davies, L., 2008: Self organisation of convection as a mechanism for memory. Ph.D. thesis, University of Reading, 173 pp.

——, R. S. Plant, and S. H. Derbyshire, 2009: A simple model of convection with memory. *J. Geophys. Res.*, **114**, D17202, https://doi.org/10.1029/2008JD011653.

——, C. Jakob, P. May, V. V. Kumar, and S. Xie, 2013a: Relationships between the large-scale atmosphere and the small-scale convective state for Darwin, Australia. *J. Geophys. Res.*, **118**, 11 534–11 545, https://doi.org/10.1002/jgrd.50645.

——, R. S. Plant, and S. H. Derbyshire, 2013b: Departures from convective equilibrium with a rapidly varying surface forcing. *Quart. J. Roy. Meteor. Soc.*, **139**, 1731–1746, https://doi.org/10.1002/qj.2065.

Del Genio, A. D., J. Wu, A. B. Wolf, Y. Chen, M.-S. Yao, and D. Kim, 2015: Constraints on cumulus parameterization from simulations of observed MJO events. *J. Climate*, **28**, 6419–6442, https://doi.org/10.1175/JCLI-D-14-00832.1.

Emanuel, K. A., 1991: A scheme for representing cumulus convection in large-scale models. *J. Atmos. Sci.*, **48**, 2313–2329, https://doi.org/10.1175/1520-0469(1991)048<2313:ASFRCC>2.0.CO;2.

Folkins, I., T. Mitovski, and J. R. Pierce, 2014: A simple way to improve the diurnal cycle in convective rainfall over land in climate models. *J. Geophys. Res. Atmos.*, **119**, 2113–2130, https://doi.org/10.1002/2013JD020149.

Grandpeix, J.-Y., and J.-P. Lafore, 2010: A density current parameterization coupled with Emanuel's convection scheme. Part I: The models. *J. Atmos. Sci.*, **67**, 881–897, https://doi.org/10.1175/2009JAS3044.1.

Guérémy, J. F., 2011: A continuous buoyancy based convection scheme: One- and three-dimensional validation. *Tellus*, **63A**, 687–706, https://doi.org/10.1111/j.1600-0870.2011.00521.x.

Held, I. M., R. S. Hemler, and V. Ramaswamy, 1993: Radiative–convective equilibrium with explicit two-dimensional moist convection. *J. Atmos. Sci.*, **50**, 3909–3927, https://doi.org/10.1175/1520-0469(1993)050<3909:RCEWET>2.0.CO;2.

Hong, S.-Y., and J.-O. J. Lim, 2006: The WRF single-moment 6-class microphysics scheme (WSM6). *J. Korean Meteor. Soc.*, **42** (2), 129–151.

Hu, Q., and D. A. Randall, 1995: Low-frequency oscillations in radiative–convective systems. Part II: An idealized model. *J. Atmos. Sci.*, **52**, 478–490, https://doi.org/10.1175/1520-0469(1995)052<0478:LFOIRC>2.0.CO;2.

Jakob, C., 2014: Going back to basics. *Nat. Climate Change*, **4**, 1042–1045, https://doi.org/10.1038/nclimate2445.

Jiménez, P. A., J. Dudhia, J. F. González-Rouco, J. Navarro, J. P. Montávez, and E. García-Bustamante, 2012: A revised scheme for the WRF surface layer formulation. *Mon. Wea. Rev.*, **140**, 898–918, https://doi.org/10.1175/MWR-D-11-00056.1.

Kuang, Z., 2010: Linear response functions of a cumulus ensemble to temperature and moisture perturbations and implications for the dynamics of convectively coupled waves. *J. Atmos. Sci.*, **67**, 941–962, https://doi.org/10.1175/2009JAS3260.1.

Liu, W. T., W. Tang, and P. P. Niiler, 1991: Humidity profiles over the ocean. *J. Climate*, **4**, 1023–1034, https://doi.org/10.1175/1520-0442(1991)004<1023:HPOTO>2.0.CO;2.

Mapes, B., and R. Neale, 2011: Parameterizing convective organization to escape the entrainment dilemma. *J. Adv. Model. Earth Syst.*, **3**, M06004, https://doi.org/10.1029/2011MS000042.

Masunaga, H., 2012: Short-term versus climatological relationship between precipitation and tropospheric humidity. *J. Climate*, **25**, 7983–7990, https://doi.org/10.1175/JCLI-D-12-00037.1.

Moncrieff, M. W., 1981: A theory of organized steady convection and its transport properties. *Quart. J. Roy. Meteor. Soc.*, **107**, 29–50, https://doi.org/10.1002/qj.49710745103.

Moseley, C., C. Hohenegger, P. Berg, and J. O. Haerter, 2016: Intensification of convective extremes driven by cloud–cloud interaction. *Nat. Geosci.*, **9**, 748–752, https://doi.org/10.1038/ngeo2789.

Pan, D.-M., and D. D. A. Randall, 1998: A cumulus parameterization with a prognostic closure. *Quart. J. Roy. Meteor. Soc.*, **124**, 949–981, https://doi.org/10.1002/qj.49712454714.

Park, S., 2014: A unified convection scheme (UNICON). Part I: Formulation. *J. Atmos. Sci.*, **71**, 3902–3930, https://doi.org/10.1175/JAS-D-13-0233.1.

Piriou, J.-M., J.-L. Redelsperger, J.-F. Geleyn, J.-P. Lafore, and F. Guichard, 2007: An approach for convective parameterization with memory: Separating microphysics and transport in grid-scale equations. *J. Atmos. Sci.*, **64**, 4127–4139, https://doi.org/10.1175/2007JAS2144.1.

Qian, L., G. S. Young, and W. M. Frank, 1998: A convective wake parameterization scheme for use in general circulation models. *Mon. Wea. Rev.*, **126**, 456–469, https://doi.org/10.1175/1520-0493(1998)126<0456:ACWPSF>2.0.CO;2.

Randall, D., and D. Pan, 1993: Implementation of the Arakawa-Schubert cumulus parameterization with a prognostic closure. *The Representation of Cumulus Convection in Numerical Models*, *Meteor. Monogr.*, No. 46, Amer. Meteor. Soc., 137–144, https://doi.org/10.1175/0065-9401-24.46.1.

——, Q. Hu, K.-M. Xu, and S. Krueger, 1994: Radiative–convective disequilibrium. *Atmos. Res.*, **31**, 315–327, https://doi.org/10.1016/0169-8095(94)90006-X.

Raymond, D. J., and M. J. Herman, 2011: Convective quasi-equilibrium reconsidered. *J. Adv. Model. Earth Syst.*, **3**, M08003, https://doi.org/10.1029/2011MS000079.

Rio, C., F. Hourdin, J.-Y. Grandpeix, and J.-P. Lafore, 2009: Shifting the diurnal cycle of parameterized deep convection over land. *Geophys. Res. Lett.*, **36**, L07809, https://doi.org/10.1029/2008GL036779.

Robe, F. R., and K. A. Emanuel, 2001: The effect of vertical wind shear on radiative–convective equilibrium states. *J. Atmos. Sci.*, **58**, 1427–1445, https://doi.org/10.1175/1520-0469(2001)058<1427:TEOVWS>2.0.CO;2.

Romps, D. M., 2011: Response of tropical precipitation to global warming. *J. Atmos. Sci.*, **68**, 123–138, https://doi.org/10.1175/2010JAS3542.1.

Rotunno, R., J. B. Klemp, and M. L. Weisman, 1988: A theory for strong, long-lived squall lines. *J. Atmos. Sci.*, **45**, 463–485, https://doi.org/10.1175/1520-0469(1988)045<0463:ATFSLL>2.0.CO;2.

Rowe, A. K., and R. A. Houze, 2015: Cloud organization and growth during the transition from suppressed to active MJO conditions. *J. Geophys. Res. Atmos.*, **120**, 10 324–10 350, https://doi.org/10.1002/2014JD022948.

Sherwood, S. C., D. Hernández-Deckers, M. Colin, and F. Robinson, 2013: Slippery thermals and the cumulus entrainment paradox. *J. Atmos. Sci.*, **70**, 2426–2442, https://doi.org/10.1175/JAS-D-12-0220.1.

Skamarock, W., and Coauthors, 2008: A description of the Advanced Research WRF version 3. NCAR Tech. Note NCAR/TN-475+STR, 113 pp., https://doi.org/10.5065/D68S4MVH.

Stephens, G. L., and Coauthors, 2010: Dreary state of precipitation in global models. *J. Geophys. Res.*, **115**, D24211, https://doi.org/10.1029/2010JD014532.

Stevens, B., and S. Bony, 2013: What are climate models missing? *Science*, **340**, 1053–1054, https://doi.org/10.1126/science.1237554.

Stirling, A. J., and J. C. Petch, 2004: The impacts of spatial variability on the development of convection. *Quart. J. Roy. Meteor. Soc.*, **130**, 3189–3206, https://doi.org/10.1256/qj.03.137.

Stratton, R. A., and A. J. Stirling, 2012: Improving the diurnal cycle of convection in GCMs. *Quart. J. Roy. Meteor. Soc.*, **138**, 1121–1134, https://doi.org/10.1002/qj.991.

Tan, J., C. Jakob, and T. P. Lane, 2013: On the identification of the large-scale properties of tropical convection using cloud regimes. *J. Climate*, **26**, 6618–6632, https://doi.org/10.1175/JCLI-D-12-00624.1.

——, ——, W. B. Rossow, and G. Tselioudis, 2015: Increases in tropical rainfall driven by changes in frequency of organized deep convection. *Nature*, **519**, 451–454, https://doi.org/10.1038/nature14339.

Tobin, I., S. Bony, C. E. Holloway, J.-Y. Grandpeix, G. Sèze, D. Coppin, S. J. Woolnough, and R. Roca, 2013: Does convective aggregation need to be represented in cumulus parameterizations? *J. Adv. Model. Earth Syst.*, **5**, 692–703, https://doi.org/10.1002/jame.20047.

Tompkins, A. M., 2001a: Organization of tropical convection in low vertical wind shears: The role of cold pools. *J. Atmos. Sci.*, **58**, 1650–1672, https://doi.org/10.1175/1520-0469(2001)058<1650:OOTCIL>2.0.CO;2.

——, 2001b: Organization of tropical convection in low vertical wind shears: The role of water vapor. *J. Atmos. Sci.*, **58**, 529–545, https://doi.org/10.1175/1520-0469(2001)058<0529:OOTCIL>2.0.CO;2.

——, and G. C. Craig, 1998: Radiative–convective equilibrium in a three-dimensional cloud-ensemble model. *Quart. J. Roy. Meteor. Soc.*, **124**, 2073–2097, https://doi.org/10.1002/qj.49712455013.

——, and A. G. Semie, 2017: Organization of tropical convection in low vertical wind shears: Role of updraft entrainment. *J. Adv. Model. Earth Syst.*, **9**, 1046–1068, https://doi.org/10.1002/2016MS000802.

Waliser, D., and Coauthors, 2009: MJO simulation diagnostics. *J. Climate*, **22**, 3006–3030, https://doi.org/10.1175/2008JCLI2731.1.

Wang, S., and A. H. Sobel, 2011: Response of convection to relative sea surface temperature: Cloud-resolving simulations in two and three dimensions. *J. Geophys. Res.*, **116**, D11119, https://doi.org/10.1029/2010JD015347.

Wang, W., and Coauthors, 2014: Weather Research and Forecasting ARW version 3 modeling system user's guide. Tech. Rep., NCAR/Mesoscale and Microscale Meteorology Division, 428 pp., http://www2.mmm.ucar.edu/wrf/users/docs/user_guide_V3.6/ARWUsersGuideV3.6.1.pdf.

Willett, M. R., and M. A. Whitall, 2017: A simple prognostic based convective entrainment rate for the Unified Model: Description and tests. Forecasting Research Tech. Rep. 617, Met Office, 53 pp., https://www.metoffice.gov.uk/binaries/content/assets/mohippo/pdf/library/frtr_617_2017p.pdf.

Wing, A. A., K. Emanuel, C. E. Holloway, and C. Muller, 2017: Convective self-aggregation in numerical simulations: A review. *Surv. Geophys.*, **38**, 1173–1197, https://doi.org/10.1007/s10712-017-9408-4.

Yano, J.-I., and R. S. Plant, 2012a: Finite departure from convective quasi-equilibrium: Periodic cycle and discharge-recharge mechanism. *Quart. J. Roy. Meteor. Soc.*, **138**, 626–637, https://doi.org/10.1002/qj.957.

——, and ——, 2012b: Convective quasi-equilibrium. *Rev. Geophys.*, **50**, RG4004, https://doi.org/10.1029/2011RG000378.